Waste Management 100 (2019) 182–190

Contents lists available at ScienceDirect

Waste Management

journal homepage: www.elsevier.com/locate/wasman

Research on synergistically hydrothermal treatment of municipal solid waste incineration fly ash and sewage sludge

Zhan Chen [a,b], Guangwei Yu [a], Yin Wang [a,*], Xuejiao Liu [a], Xingdong Wang [a]

[a] CAS Key Laboratory of Urban Pollutant Conversion, Institute of Urban Environment, Chinese Academy of Sciences, Xiamen 361021, China
[b] University of Chinese Academy of Sciences, Beijing 100049, China

ARTICLE INFO

Article history:
Received 2 June 2019
Revised 2 September 2019
Accepted 6 September 2019

Keywords:
IFA
Sludge dewatering
HTT
Chlorine migration
HM immobilization

ABSTRACT

To explore a feasible method of utilizing municipal solid waste incineration fly ash (IFA) rather than releasing it into solidified landfill, in this work, IFA was pretreated by mixing it with municipal sewage sludge (MSS) and applying hydrothermal treatment (HTT). The influences of the IFA dosage, HTT temperature, HTT time, and liquid to solid ratio (L/S) on the dewatering, chlorine migration, solidification, and leaching of heavy metals (HMs) in MSS were investigated. The results show that the synergistic effect was obtained, IFA enhanced the dewatering of MSS and in return, MSS improved the release of chlorine in IFA. The optimal pretreatment conditions were an IFA dosage of 5%, HTT temperature of 180 °C and HTT time of 60 min. The moisture of the solid residue after HTT could be controlled below 40%. Under a fixed IFA dosage, the chlorine content of the liquid could be reached almost 50% with increasing HTT temperature, and the chlorine distribution exhibited a strong positive correlation with the L/S ratio ($R^2 > 0.90$). The migrating chlorine was mainly derived from its soluble state, which was controlled by the HTT liquid volume. After the soluble chlorine was dissolved, bound chlorine compounds, such as CaCl(OH), gradually neutralized and released chlorine into the liquid during HTT, and finally reached an equilibrium as the L/S ratio continued to increase. In addition, during HTT, satisfactory HM immobilization performance was achieved and the fraction of HMs, such as Cr, Ni, Cu and Zn, stabilized.

1. Introduction

Owing to its superiority in terms of mass and volume reduction, and heat and electricity production (Pan et al., 2013), incineration is gradually being applied to treat MSW worldwide. However, a large amount of incineration fly ash (IFA) and bottom ash was produced in the process. Bottom ash, which can be applied without treating or less treating (Jing et al., 2013), could be realized reuse. For example, (Ashok et al., 2018) used bottom ash as catalytic support for biomass tar reforming, improving toluene conversion and reducing coke formation. As IFA absorbs large amounts of soluble salts(Yang et al., 2017), organic matters (POPs) (Weidemann and Lundin, 2015) and toxic HMs (Youcai, 2017), it severely impacts the environment and human health, and is listed as a hazardous waste (HW18: a code of IFA). Therefore, it is vital that technologies are developed for safely treating and disposing of IFA.

The current IFA treatment technologies include acid extraction and separation (Tang et al., 2018), solidification and stabilization (Qian et al., 2006), using it as a cement additive (Lederer et al., 2017), and thermal treatment (Yin et al., 2013). However, there may be some problems in practice. For example, acid washing produces a large amount of wastewater, solidification and stabilization require the addition of a chemical reagent and cement, and ash fusion requires more energy. As a cement additive, the existing chlorine in IFA would decrease the strength of the material and corrode equipment. Thus, further exploration of methods to improve energy-saving and efficiency is required.

As an emerging method, hydrothermal treatment (HTT) has been applied successfully in methods of IFA disposal, particularly detoxification (Xie et al., 2010) and solidification (Jin et al., 2012). In (Hu et al., 2012) research, considerable high efficiencies of dioxin decomposition and HMs stabilization in IFA were achieved during HTT with a mixture of ferric sulphate and ferrous sulphate serviced as the reactant. An investigation of the effect of HTT on HMs in IFAs from a circulating fluidized bed (CFB) and stoker grate

Abbreviations: MSW, municipal solid waste; IFA, incineration fly ash; MSS, municipal sewage sludge; HTT, hydrothermal treatment; L/S, liquid to solid ratio; HMs, heavy metals; POPs, persistent organic pollutants; CFB, circulating fluidized bed; APC, air pollutant control; CST, capillary suction time; IC, ion chromatography; ICP-MS, inductively coupled plasma mass spectrometry; TCLP, toxicity characteristic leaching procedures; COD, chemical oxygen demand.

* Corresponding author at: Institute of Urban Environment, Chinese Academy of Sciences, Xiamen 361021, China.
E-mail address: yinwang@iue.ac.cn (Y. Wang).

https://doi.org/10.1016/j.wasman.2019.09.006
0956-053X/

demonstrated that HM species become more stable after HTT, and the content of HMs in leachate decreased (Jin et al., 2012). (Hu et al., 2015) compared the effects of IFA and the acid washing of IFA on HMs, and found that acid washing could improve the release of HMs and the addition of ferric/ferrous or phosphate further stabilized the following process. Many researchers have utilized water washing to achieve a high chlorine removal rate from IFA, and the liquid to solid ratio (L/S), washing retention time, and frequency have been widely studied (Chen et al., 2016; Wang et al., 2010; Yang et al., 2017). However, this process usually consumes a high amount of clean water and produces large amounts of high-salinity wastewater, causing issues in post-processing.

However, the production of MSS, the byproduct of wastewater treatment plants, in China is rapidly increasing (Zhang et al., 2017). Some of the difficulties faced in the disposal of MSS disposal are its high moisture content and viscosity. Therefore, the dehydration of MSS has continued to be of great interest in recent years (Ye et al., 2017). For example, (Qiao et al., 2010) reported a reduction in the water content of dewatered cake from 80% to 50% with hydrothermal conditioning at 170 °C. (Wang et al., 2014) also studied MSS dewatering using HTT coupled with mechanical expression, and suggested that the HTT temperature was a vital factor and explained the dehydration mechanism from the perspective of the structure of MSS cells. In addition, they also compared the energy demand of thermal drying and electro-dewatering, and concluded that HTT is an energy-saving dehydration process. To further enhance dehydration and reduce the cost, chemicals, such as alkaline solvents, have also been added to HTT (Li et al., 2017). HTT could also immobilize the HMs in MSS. (Liu et al., 2018) reported that HMs accumulate in hydrothermal residues, reducing their content in leachate. (Wang et al., 2016a) also investigated the HMs in hydrochar used as a soil conditioner and conducted an environmental assessment, and found that HTT significantly mitigated the environmental risk of HMs.

The multiple components of IFA are beneficial to MSS dehydration, and the high moisture content of MSS can dissolve the hazardous chlorines in IFA and significantly reduce the clean water consumption. Moreover, this synergistic treatment process can further decrease the environmental risk. (Zhang et al., 2011) mixed 97% MSS with different dosages of IFA for dewatering, and found that pH and chlorine could promote MSS dehydration. (Hu et al., 2018) used IFA and MSS to immobilize HMs via pyrolysis and also achieved satisfactory HMs immobilization. However, no studies have systematically investigated the synergistic chlorine migration regularity in IFA and the dewatering behavior of MSS in the mixed HTT system.

In this study, IFA mixed with MSS was pretreated by HTT to explore a feasible method of utilizing IFA instead of sending it for disposal in solidified landfill. IFA dosage was chosen as a key factor because it would not only impact Cl distribution and migration, also promote MSS dehydration during synergistically HTT of IFA and MSS. Based on the prerequisite of the optimal IFA dosage, the main process parameters - HTT temperature and HTT time were chosen to investigate the influence on Cl migration, MSS dehydration and HMs immobilization. For further study of the migration regulation of Cl, the factor of L/S was also chosen and systematically investigated, so as to provide some references in future practically application.

2. Materials and methods

2.1. IFA and MSS samples

IFA samples were obtained from a stoker grate MSW incineration plant in Xiamen, which has a capacity of 800 ton d^{-1}. The incinerator is equipped with air pollutant control (APC) apparatus, including a dry scrubber, an activated carbon injector, and a fabric filter.

The MSS samples were obtained from a wastewater treatment plant in Xiamen, China, which has a treatment capacity of 10.000 m^3 d^{-1} and applies the oxidation-ditch process. The MSS was been condensed by gravity and a belt filter before collection and had a moisture content of 83.14%. The samples were stored in a refrigerator at 4 °C before use.

The main components of the samples determined through elemental and proximate analysis are listed in supplemental materials (SM-Table 1). MSS had a higher moisture content of over 80%, and the content of volatiles on a dry basis was also almost 50%, indicating that the MSS contained large amounts of organic matters. Furthermore, according to the ultimate analysis, the carbon content exceeded 25%. The contents of chlorine, sodium, and potassium in the IFA were much higher than those in the MSS. The higher chlorine content was due to the high contents of PVC and kitchen waste in MSW, thus, some chloric compounds with a low-boiling point condensed on the surface of the fly ash during the APC process after incineration (Qi et al., 2018). Furthermore, the calcium content was relatively large because calcium hydroxide was used to absorb the acid gas in the flue gas.

Zn and Pb are more volatile than the other HMs (Nowak et al., 2012), and first and second most abundant HMs in IFA. The content of individual HMs in IFA decreased in the following order: Zn > Pb > Cu > Cr > Cd > Ni. The HM contents of MSS greatly differed, with Cr, Cu, and Zn serving as the most abundant HMs, with a total amount of almost 5,000 ppm. Specific information regarding the HMs is listed in SM-Table 1.

2.2. HTT apparatus and procedures

All batch HTT experiments were conducted using a SUS316L autoclave with a capacity of 1 L equipped with a central electrical stirrer. For each experiment, certain amounts of MSS (raw or dried), IFA, and deionized water were mixed thoroughly and added to the reactor, and the L/S ratio of the mixture ranged from 3 to 12. During HTT, the temperature was set to increase from 120 to 240 °C with a heating rate of 5 °C/min, and the holding time was changed from 30 to 120 min by uninterrupted stirring. The pressure varied with the temperature during the experiments. The detailed experimental control parameters were presented in Table 1 and univariate analysis method was used to optimize HTT parameters. From No. 1 to No. 5, the effect of IFA dosage was mainly investigated; from No. 6 to No. 10 the influence of HTT temperature was explored; the effect of HTT time was showed from No. 11 to No. 14. The experiments from No. 15 to No. 21 were designed for explaining Cl migration regulation with L/S changing.

Following HTT, the autoclave was cooled to room temperature using water. The products were transferred to a 1-L beaker, and the capillary suction time (CST) of the mixtures was detected to assess the dewatering performance. The mixture was then filtered by vacuum filtration and the filter cake obtained was dried at 105 °C in an oven to measure the moisture content. After drying, the residues were stored in a desiccator prior to further analysis. The filtrate was filtered through a 0.22-μm filter membrane and the pH of the filtrate was measured using a pH meter (Mettler Toledo FE20). The filtrate was then stored in a refrigerator at 4 °C for other analyses.

2.3. Analytical methods

2.3.1. Composition and structure analysis

The CHNS analysis of the MSS, IFA, and HTT residues was conducted using an elemental analyzer (Analytik Jena multi® EA

Table 1
HTT conditions.

No.	HTT temperature (°C)	HTT time (min)	L/S ratio (-)	MSS (g)		IFA (g)	DI water (ml)
				Raw	Dried		
1	180	60	–	500	–	0	100
2	180	60	–	500	–	15	100
3	180	60	–	500	–	25	100
4	180	60	–	500	–	35	100
5	180	60	–	500	–	50	100
6	120	60	1:4	500	–	25	100
7	150	60	1:4	500	–	25	100
8	180	60	1:4	500	–	25	100
9	210	60	1:4	500	–	25	100
10	240	60	1:4	500	–	25	100
11	180	30	1:4	500	–	25	100
12	180	60	1:4	500	–	25	100
13	180	90	1:4	500	–	25	100
14	180	120	1:4	500	–	25	100
15	180	60	1:3.2	500	–	25	0
16	180	60	1:4	500	–	25	100
17	180	60	1:6.4	250	–	12.5	200
18	180	60	1:8	250	–	12.5	300
19	180	60	1:8	–	20	5	200
20	180	60	1:10	–	20	5	250
21	180	60	1:12	–	20	5	300

2000), the chemical composition of raw materials was determined using an x-ray fluorescence spectrometer (XRF, S4-Explore, Bruker), and the crystalline structure of the samples was determined using an x-ray diffractometer (XRD, Rigaku Rotaflex). The program parameters can be found in our previous report (Liu et al., 2019). The functional groups of the hydrothermal residues were characterized using their Fourier transform infrared (FTIR) spectra, and the operation procedure for this was described in our previous study (Wang et al., 2019).

2.3.2. Chlorine analysis

The chlorine content of the filtrate was measured using ion chromatography (ICS---3000, America). The total chlorine content of the samples was determined following a thermal method combined with ion chromatography (IC, DIONEX, CS-2500). The total amount of chlorine (W_i, μg/g) in the raw material can be calculated by Eq. (1).

$$W_i = \frac{C_i \times V_i \times D_i \times 10^3}{M_i} (i = 1, 2) \quad (1)$$

where i is 1 or 2 and represents the chlorine in MSS or IFA, respectively; C_i is the concentration measured by IC, mg/L; V_i is the solution volume, L; D_i expresses the dilution factor; and M_i is the weight of the MSS or IFA, g.

The liquid distribution of chlorine after HTT was expressed as ω (%) and can be calculated by Eq. (2)

$$\omega = \frac{C_t \times V_t \times D_t}{\sum_{i=1}^{2} W_i \times M_i} \times 100\% \quad (2)$$

where C_t is the chlorine concentration in the HTT liquid after the experiment, mg/L; V_t is the volume of liquid, L; and D_t is the dilution factor.

2.3.3. Heavy metals analysis

The total amount of HMs in the residues and samples was measured by inductively coupled plasma mass spectrometry (ICP-MS, XSERI, Thermo Scientific) after digestion in a mixed acid (HNO3: HF: HClO4 = 5:5:2) system assisted by microwave power (EXCEL, PreeKem).

Toxicity characteristic leaching procedures (TCLPs) were conducted following US EPA standard 1990. First, 1 g of the dried residue sample was ground to a size of less than 200 μm and was then subsequently extracted using an acetic acid solution (pH 2.88) at a L/S ratio of 20:1. Second, the mixture was shaken in a horizontal oscillator for 18 ± 2 h at a speed of 200 rpm. Finally, the suspensions were filtered through a 0.22-μm membrane and analyzed by ICP-MS.

Furthermore, a three-step BCR sequential extraction procedure was conducted to determine the distribution of HM species before and after HTT. Four fractions were recognized: a sequential acid-soluble/exchangeable fraction (F1), a reducible fraction (F2), an oxidizable fraction (F3), and a residual fraction (F4). The specific extraction procedure was described in our previous study (Wang et al., 2016b).

2.4. Quality assurance and quality control

All measurements in our experiments were collected three times, and the average values and error bars were utilized to ensure.

3. Results and discussion

3.1. Dewatering performance of MSS during HTT

IFA contains some components effective in MSS dewatering, such as calcium and chlorine compounds (Zhang et al., 2011). Hence, a mixture of MSS and IFA underwent HTT, and the dewatering behavior of MSS affected by IFA was investigated.

In this study, the HTT temperature and time were maintained at 180 °C and 60 min, respectively. Fig. 1 shows that adding IFA to MSS improved MSS dehydration, as the moisture content of MSS decreased with the IFA dosage. For example, when the percentage of IFA was 5.0%, the moisture content of MSS after HHT decreased from the initial value of 44.43–36.25%, and the capillary suction time (CST) decreased from its initial value of 25.1–12.0 s. The calcium hydroxide or calcium carbonate in IFA could destroy the cell wall of MSS, freeing the binding water under alkaline conditions (Li et al., 2017). Additionally, chlorine in IFA could cause microbe cells to shrink and enhance the dewatering performance. However, when the amount of added IFA was increased from 5% to 10%, there was only a slight improvement in MSS dewatering. Moreover, the

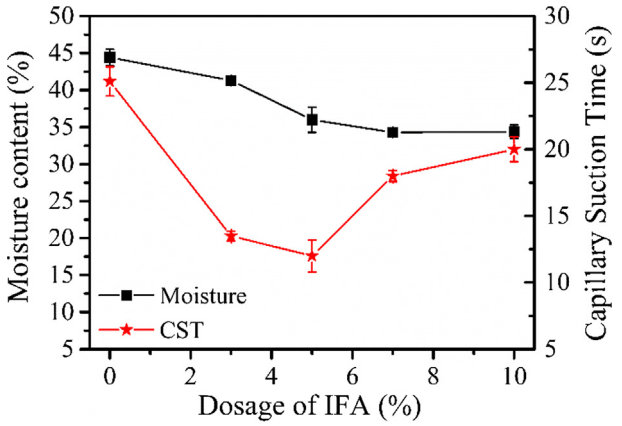

Fig. 1. Effect of IFA dosage on MSS dewatering during HTT (T = 180 °C, t = 60 min).

CST increased from 12.0 to 20.0 s, indicating that the filtration efficiency decreased. Therefore, an IFAA dosage of 5% was chosen for this work.

It has been reported that temperature is a key factor in HTT (Kumar et al., 2018), as it determines the treatment efficiency and cost. Furthermore, the HTT time influences the treatment capacity. Thus, the effects of HTT temperature and time on MSS dewatering are investigated in depth in this section.

Fig. 2a shows that the HHT temperature had significantly affected MSS dewatering, particularly between 120 and 180 °C. For example, when the temperature was 120 °C, the moisture content of MSS was 51.30%, while the moisture content decreased to 39.70% at a temperature of 180 °C. Correspondingly, the capillary suction time (CST) decreased from its initial value of 988.2 s to 15.2 s. However, the moisture content of MSS slightly decreased when the HHT temperature increased from 180 to 240 °C. This could be explained by the disaggregation of sludge flocculates. Generally, with an elevation in the reaction temperature during HTT, the structures of microbe cells, including the hydrocarbons, proteins, and lipase, are destroyed and the binding water in MSS is released (Yu et al., 2014). This could also be indirectly verified by the changes in the contents of the CHN elements in residues and chemical oxygen demand (COD), which was detected using a COD Rapid Tester (Tsinghua technical), in the liquid during HTT. With an increase in the HTT temperature from 120 to 240 °C, the contents of C, H, and N in the solid residues (SM Table 2) declined from 21.44 to 17.98%, 3.51 to 1.99%, and 3.16 to 2.49%, respectively. However, the COD in the HTT liquid increased from 28.89 to 42.31 g/L (SM Table 2).

The HTT time had no notable effect on MSS dewatering (Fig. 2b). Even with an increase in the reaction time to 120 min, the moisture content only slightly decreased from 40.14 to 38.23%. It was found that the CST greatly decreased before 60 min, and then continued to slightly decrease until 120 min. This could be due to the completion of the hydrothermal reaction within 60 min, and the release of more free water. With a continuous increase in HTT time, refractory matter began to gradually degrade and the CST slowly decreased after 90 min. Furthermore, a longer reaction time would increase the energy input, decrease the treatment capacity, and increase the running costs.

According to the above results, a temperature of 180 °C and time of 60 min are satisfactory HTT conditions for MSS dewatering under the synergistic treatment of IFA and MSS.

3.2. Distribution of chlorine during HTT

3.2.1. Effects of HTT temperature and time on chlorine migration

The chlorine in IFA accounts for a large proportion of the ash and can corrode equipment or participate in the transformation of dioxin. Thus, the chlorine migration regularity during the synergistic HTT of IFA and MSS needs to be explored and the optimal parameters for chlorine control in practice must be determined.

First, the primary forms of chlorine in IFA and MSS were confirmed by XRD, which could be found in supplemental materials (SM-Fig. 1). It shows that the main forms of chlorine in IFA included KCl, NaCl, and CaCl(OH), which were in conformance in a previous report (Zhu et al., 2008). However, they also reported that some insoluble forms of chlorine, such as Friedel's salt, exist in IFA, which differed to our results (SM-Fig. 1a). The content of insoluble chlorine in our materials may have been relatively low and no notable peak was observed. No clear peak indicating the presence of chlorine compounds was observed in the XRD pattern of MSS (SM-Fig. 1b). This might because the chlorine content of MSS was significantly lower than that in IFA. Therefore, it was not detected by XRD. Another explanation for this is that the chlorine in MSS combines with mineral, therefore, the soluble chlorine was mainly derived from IFA during the synergistic HTT of IFA and MSS.

The effects of HTT temperature and time on chlorine migration between the solid residue and liquid phase were then investigated. Fig. 3a shows that the chlorine dissolved into the liquid phase increased as the HTT temperature increased to 210 °C. For example, at a temperature of 120 °C, the chlorine content of the HTT liquid phase was only 21.41%, while it increased to almost 47.80% at 210 °C. This can be explained as follows. First, with an increase in HTT temperature, the hydrothermal reaction becomes intense and

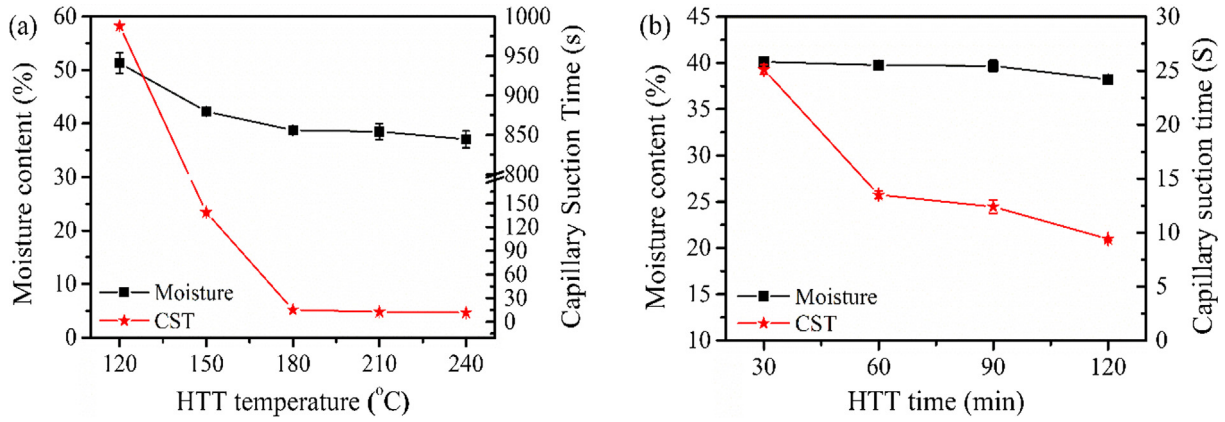

Fig. 2. Effect of temperature and time on MSS dewatering during HTT (a, t = 60 min, IFA = 5%; b, T = 180 , IFA = 5%).

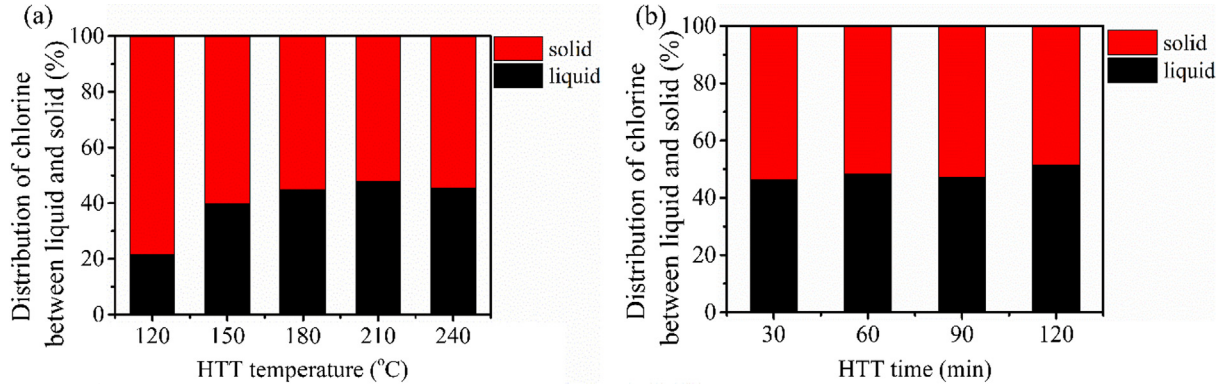

Fig. 3. Distribution of chlorine in the HTT liquid and solid residue under different conditions (a, t = 60 min, IFA = 5%; b, T = 180 °C, IFA = 5%).

the dewatering efficiency is enhanced, leading to an increase in the volume of HTT liquid, causing more of the soluble chlorines, such as KCl, NaCl, and $CaCl_2$, in IFA to dissolve into the liquid phase, as described in Eqs (3)–(5). Second, organic acid (R-COOH) accumulated as the experimental temperature increased due to the increase in the number of microbial cells in the MSS, resulting in the neutralization of some persistent chlorine compounds, such as CaCl(OH), by these acidic compounds, further promoting the migration of chloric compounds into the HTT liquid, as expressed by Eq. (6).

$$NaCl(s) + H_2O \rightarrow NaCl(aq) \quad (3)$$

$$KCl(s) + H_2O \rightarrow KCl(aq) \quad (4)$$

$$CaCl_2(s) + H_2O \rightarrow CaCl_2(aq) \quad (5)$$

$$CaCl(OH) + R - COOH(aq) \rightarrow RCOO - Ca + H_2O(l) + Cl^- \quad (6)$$

$$OH^- + R - COOH(aq) \rightarrow RCOO^- + H_2O(l) \quad (7)$$

$$Ca(OH)_2(s) + CO_2(g) \rightarrow CaCO_3(s) + H_2O(l) \quad (8)$$

However, HTT time did not greatly influence the distribution of chlorine between the liquid and solid phase under a constant HTT temperature of 180 °C (Fig. 3b). Therefore, the HTT time might not be the main factor affecting the process of chlorine migration.

To verify the above discussion, the XRD patterns of the solid residues after HTT were compared. As shown in Fig. 4, the peaks of soluble salts, such as $CaCl_2$ and KCl, appeared to disappear completely in the XRD patterns as the HTT temperature increased. However, the peak indicating the presence of NaCl still existed in the patterns of the residues, even after treatment at 240 °C. This might be because the amount of NaCl in IFA was much higher than that of KCl and $CaCl_2$ (SM-Table 1), and the volume of liquid phase after HTT was not sufficient to completely dissolve all of the NaCl. However, the peaks of $Ca(OH)_2$ and CaCl(OH) in the XRD patterns of raw MSS and IFA disappeared after HTT. (Berge et al., 2011) reported that, apart from the production of organic acid, decarboxylation would also occur with an increase in temperature increase during MSS HTT. All of these processes would consume OH^-, as described by Eqs. (7) and (8). Therefore, the OH^- functional group in the mixture of MSS and IFA disappeared after HTT. This can also explain the decrease in the pH of the HTT liquid from 9.65–8.95 during HTT (SM-Table 2). However, above 210 °C, the pH increased slightly due to the release of ammonia in protein.

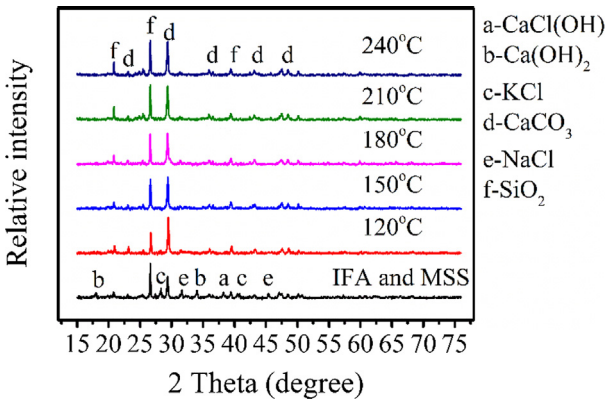

Fig. 4. XRD patterns during the synergistic HTT of IFA and MSS under different temperatures. (t = 60 min, IFA = 5%).

3.2.2. Effect of L/S ratio on chlorine migration

The above discussion shows that the volume of HTT liquid affected the soluble chlorine compounds. When the HTT liquid volume was lower, the proportion of chlorine in the liquid phase was smaller, while the concentration of chlorine was higher. This would also pose a significant risk of corrosion to the hydrothermal equipment. Therefore, the effects of the L/S ratios during the synergistic HTT of IFA and MSS, including raw MSS and dried MSS, were explored. The L/S ratio ranged from 3.2:1 to 8:1 for raw MSS, and 8:1 to 12:1 for dried MSS. The detailed experimental parameters are listed in Table 1 and the chlorine migration regulations are presented in Fig. 5.

There was a great difference in the migration efficiency of chlorine in IFA with different forms of MSS. Generally, the percentage of chlorine in the liquid phase was higher for IFA and dried MSS than that for IFA and raw MSS, even with the same L/S ratio. For the IFA and raw MSS system, the efficiency of chlorine transformation from the solid phase to the liquid phase almost increased linearly with the L/S ratio. For example, the percentage of chlorine in the liquid phase after HHT increased from 40 to 60% when the L/S ratio changed from 3.2:1 to 8:1. As the soluble salt content was too high, such as Na and Cl, the limited solution would become saturated very rapidly at a low L/S ratio. As the L/S ratio increased, more HTT liquid would be produced, causing these soluble compounds to continue to dissolve. Therefore, the migration efficiency of chlorine between the solid and liquid phases was controlled by the volume of liquid.

A slow variation tendency for chlorine transformation was achieved during the synergistic HTT of IFA and dried MSS. The percentage of chlorine in the liquid phase increased from 65 to 70% as

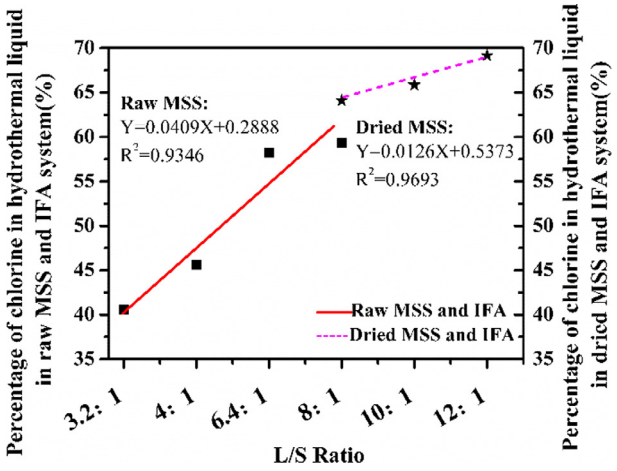

Fig. 5. Effect of L/S ratio on chlorine migration during the synergistic HTT of IFA and different forms of MSS (T = 180 °C; t = 60 min; MSS/IFA ratio = 4/1, dry weight).

the L/S ratio changed from 8:1 to 12:1. This might be due to the following reasons. The water was in a free state in this system, causing thorough mixing and contact between the IFA and MSS. The soluble chlorine on the surface of the IFA particles rapidly dissolved at the beginning of HTT (Kirby and Rimstidt, 1994). After this, chlorine enters a bonded state, forming compounds such as CaCl(OH) or Friedel's salt, and would react or neutralize as the synergistic HTT continued, gradually migrating into the liquid phase. This could be verified by FTIR, which involved subtracting the background and correcting the baseline (SM-Fig. 2). From the change in transmittance, it was found that, at the wavenumber of 3500 cm^{-1}, the number of —OH functional groups slightly increased with the L/S ratio. This may be related to chlorine conversion, as the chlorine was replaced by hydroxyl and released into the liquid under a higher L/S ratio during synergistic HTT. (Chen et al., 2012) stated that, at a L/S ratio of 10:1, water-flushing can almost completely remove water-soluble chloride (97% chloride removal efficiency). Furthermore, (Zhu et al., 2009) reported that the insoluble Friedel's salt was slowly released during IFA washing. From the above analysis, it could be concluded that chlorine migration might be mainly limited by the presence of its insoluble form in this system.

Finally, the univariate linear regression equation was fitted using the experimental data under different L/S ratios. Fig. 6 shows, regardless of the form of MSS, synergistic HTT exhibited good linearity for chlorine conversion, as both R^2 values exceeded 0.90. Based on the regulation of chlorine migration, we could speculate that, for the synergistic HTT of IFA and raw MSS, the efficiency of chlorine migration in the HTT liquid would increase with a continuous increase in the L/S ratio; once the soluble chlorine dissolved completely at a certain L/S ratio, the insoluble chlorine compounds, such as CaCl(OH) or Friedel's salt, would be neutralized and released, eventually reaching an equilibrium at a higher L/S ratio ($L/S \geq 20$).

In summary, the L/S ratio greatly affected chlorine migration during the synergistic HTT of IFA and MSS in this system. However, increasing the amount of the liquid solution would increase the consumption of clean water and the production of wastewater, which would increase the burden on subsequent wastewater treatment. In this study, a L/S ratio of 6.4 (including the water bonded in the MSS) could achieve satisfactory chlorine removal during the synergistic HTT of IFA and raw MSS with low clean water consumption. Therefore, in practice, all factors should be comprehensively considered.

3.3. Distribution and leaching of HMs

Similar to chlorine, the content and leaching of HMs in the dewatered residue would also affect its subsequent reuse after the synergistic HTT of IFA and MSS. Therefore, the immobilization and distribution of HMs are investigated in the following discussion. As the contents or toxicity of Cr, Ni, Cu, Zn, Cd, and Pb were highest, they were selected as the target HMs.

SM-Table 2 indicates that the HMs in the residues tended to accumulate as HTT proceeded and the temperature increased from 120 to 240 °C. For example, the content of Cr was 3885 mg/kg at 120 °C, which increased to 4950 mg/kg at 240 °C, an increase of approximately 1000 mg/kg. Furthermore, the content of Ni increased from 573 to 734 mg/kg with the same increase in temperature. After HTT, the total amount of Cu had increased by approximately 1350 mg/kg, and the increase in the content of Zn was highest, with an increment of approximately 2000 mg/kg. As the contents of Cd and Pb in MSS were small, after the synergistic HTT of IFA and MSS, they were diluted and their contents were smaller than those in IFA. Their contents exhibited relatively small increments of 8 and 138 mg/kg, respectively. These changes could be ascribed to mass reduction. As IFA contains a high amount of soluble compounds, they would migrate into the liquid phase during synergistic HTT and the organic substances in MSS would decompose.

The variations in the total amounts of HMs with changes in HTT time were smaller than the variations with changes in HTT temperature. For example, when the HTT time increased from 30 to 120 min, the total amounts of Cr, Ni, Cu, Zn, Cd, and Pb increased by approximately 500, 130, 1300, 320, 6, and 30 mg/kg, respectively. Furthermore, there were no changes in the solid contents of the HTT products. Thus, the effect of HTT time on the accumulation of HMs was indistinctive during the synergistic HTT of IFA and MSS.

As large amounts of HMs accumulated in solid residues after HTT, their leaching behaviors were measured (Table 2) and the results show that the leaching contents of most of the HMs, including Cr, Cu, Zn, and Cd, decreased with increasing HTT temperature, which is consistent with the results of other studies (Huang and Yuan, 2016). Specifically, the leaching content of Cr reduced from 15 to 4.6 mg/kg when the HTT temperature increased from 120 to 240 °C. The contents of Cu and Cd decreased by 0.52 and 1.15 mg/kg within the range of HTT temperature, while that off Zn decreased by over 100 mg/kg due to the migration of its soluble state. However, the behavior of Ni appeared to be irregular; the leaching content increased with HTT temperature. For example, the leaching content increased from 60 to 76 mg/kg with an increase in HTT temperature from 120 to 240 °C. This is likely related to its mobility during synergistic HTT. Nevertheless, HTT time had little influence on the leaching contents of the HMs, as the variations in the amounts of the HMs were within 5 mg/kg, excluding those for Zn and Ni.

To further investigate the reason for the variation in HM leaching behaviors under different HTT temperatures, their fractions were extracted using the modified BCR technique (Fig. 6). Based on the difference in the weights of the HMs between IFA and MSS, three groups were classified. The first group contained Cr, Cu, and Ni, the contents of which were smaller in IFA than those in MSS. Thus, the migration of the HMs in this group largely relied on MSS. Specifically, fractions F3 and F4 accounted for 99% of the content of Cr in MSS, and 75% in IFA. After synergistic HTT, fractions F3 and F4 were still present. Therefore, the addition of IFA did not affect the species of these HMs in MSS, but their forms in IFA were diluted or immobilized. The distribution of Cu in MSS was similar to that of Cr. The percentages of F1 and F2 were below 5%, while F3 occupied a large share of Cu. However, in IFA, only

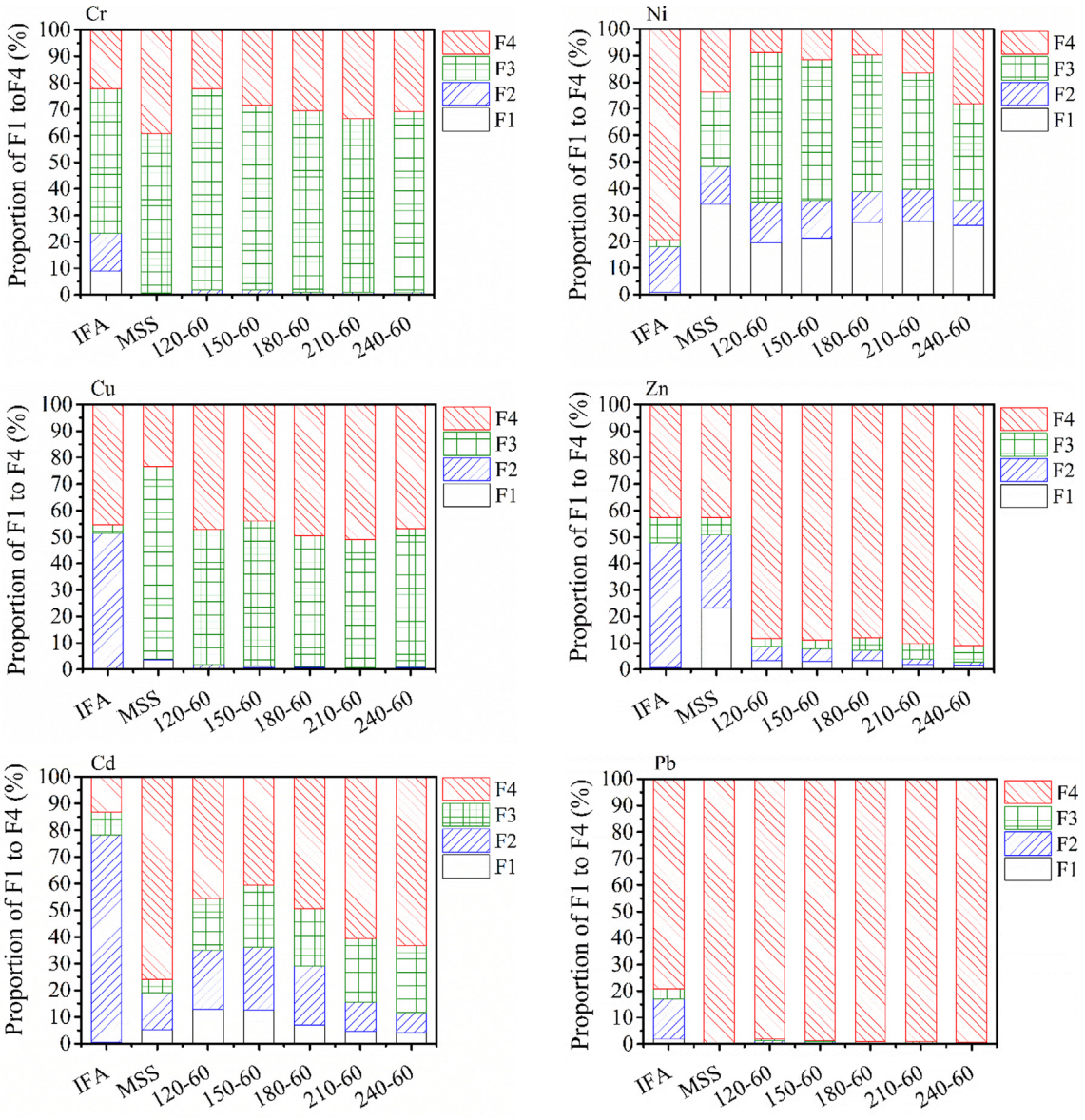

Fig. 6. Speciation of HMs under different temperatures (L/S = 1:4) (t = 60 min, MSS/IFA = 4/1, dry basis).

Table 2
Leaching concentrations in residues before and after HTT.

Samples	Cr (mg kg^{-1})	Ni (mg kg^{-1})	Cu (mg kg^{-1})	Zn (mg kg^{-1})	Cd (mg kg^{-1})	Pb (mg kg^{-1})
IFA	4.31 ± 0.46	0.34 ± 0.02	1.47 ± 0.35	8.10 ± 0.02	0.63 ± 0.16	39.46 ± 2.35
MSS	17.22 ± 1.87	141.63 ± 14.43	6.56 ± 0.07	441.23 ± 0.19	0.38 ± 0.05	2.36 ± 0.10
120–60*	15.39 ± 0.73	60.18 ± 2.57	7.46 ± 0.39	192.14 ± 0.20	2.21 ± 0.21	0.95 ± 0.12
150–60	13.14 ± 0.64	67.66 ± 0.48	6.99 ± 0.28	172.59 ± 0.09	1.94 ± 0.01	ND
180–60	7.85 ± 0.43	61.52 ± 0.44	6.82 ± 0.21	156.31 ± 0.07	1.83 ± 0.00	ND
210–60	5.98 ± 0.03	73.84 ± 0.83	7.01 ± 1.01	106.89 ± 0.17	1.20 ± 0.04	ND
240–60	4.62 ± 0.19	76.39 ± 2.31	6.94 ± 0.30	74.70 ± 0.11	1.06 ± 0.05	ND
180–30	10.09 ± 0.99	62.42 ± 1.45	7.14 ± 3.25	157.10 ± 5.46	1.87 ± 0.01	ND
180–60	7.85 ± 0.43	61.52 ± 0.44	6.82 ± 0.21	156.31 ± 0.07	1.83 ± 0.00	ND
180–90	7.07 ± 0.57	69.24 ± 0.57	6.43 ± 0.14	153.72 ± 14.76	1.76 ± 0.08	ND
180–120	6.87 ± 0.55	69.13 ± 5.52	6.59 ± 0.73	139.50 ± 5.89	1.75 ± 0.05	ND
	GB5085.3-2007					
Standard	15.00	5.00	100.00	100.00	1.00	5.00

* , 120–60: HTT temperature and HTT time, respectively. ND: no detection

fraction F2 accounted for a proportion of over 50%. After synergistic HTT, F3 and F4 were predominant, accounting for over 98% of the Cu. Therefore, HTT shifted the content of Cu from F2 to F3 and F4, enhancing the immobilization of HMs. Finally, for Ni, the shares of fractions F1 and F2 in MSS exceeded 50%, but the share of F3 gradually increased as HTT proceeded. This is because Ni is a good

organic ligand, and entered organic bonds after the HTT of MSS (Wang et al., 2019).

The second group included Pb and Cd, which mainly originated from IFA. For Pb, the proportions of F1 and F2 in IFA were high, approaching 20%. After HTT, Pb stabilized, mainly existing as F4, which accounted for over 98% of Pb, even at a low HTT temperature. Therefore, MSS improved the immobilization of Pb during HTT. This might be due to the following. As HTT proceeded, the carbon dioxide produced from the MSS and the Pb in IFA reacted with and immobilized Pb. The percentages of F1 and F2 in Cd were almost 80% in IFA and 20% in MSS. Thus, the leaching content of Cd was high in raw IFA. After HTT, the fractions of F1 and F2 decreased to 40% at 120 °C and fell below 10% at 240 °C. Meanwhile, the fractions of F3 and F4 increased, indicating that the amount of released Cd decreased after HTT.

The third group was Zn, which was affected by both MSS and IFA as it exhibited the smallest weight difference between MSS and IFA. Fraction F1 fraction accounted for 20% of the Zn in MSS, while F1 and F2 accounted for almost 50%. However, in IFA, F1 was very small and F2 accounted for 50%. After HTT, Zn migrated from F1, F2, and F3 to F4. This result was in accordance with a previous report (Zhai et al., 2016), that stated that the alkaline reaction environment during the HTT of MSS could improve the retention and immobilization of HMs in the hydrochar. As IFA has high alkalinity, the immobilization of HMs was enhanced.

In summary, HTT exhibited a good HM immobilization efficiency during the synergistic treatment of IFA and MSS, as HMs were transformed from a soluble state into a stable form. Under HTT conditions of 240 °C and 60 min, most HMs, excluding Ni and Cd, met the leaching standards of HMs in GB5085.3-2007. If the total amount of HMs is considered, the environment could be impacted. Necessary measures should be taken for the post-treatment extraction and reuse of residue in practice.

4. Conclusion

Experiments were conducted on the synergistic HTT of IFA and MSS with variations in the treatment parameters, including the dosage of IFA, HTT temperature, HTT time, and solid to liquid ratio. The dehydration of MSS, chlorine migration of IFA, and HMs immobilization in the system were analyzed and the show that adding IFA could create a high pH and calcic environment, promoting the degradation of MSS microbes and enhancing the MSS dewatering efficiency. Under an IFA dosage of 5%, the ideal HTT conditions are a temperature of 180 °C and time of 60 min, which would control the moisture content within 40%.

The HTT temperature and L/S played important roles in regulating the migration of chlorine during the synergistic HTT of IFA and MSS. Under a fixed IFA dosage, as the temperature increased, the percentage of chlorine in the liquid phase increased. Within a limited scope, the L/S ratio has a strong positive correlation with the process of chlorine migration ($R2 > 0.90$) with both raw or dried MSS. The conversion of chlorine included two steps during the co-HTT of IFA and MSS. First, chlorine was mainly derived from the soluble state, which was controlled by the volume of HTT liquid. Following this, bound forms of chlorine, such as CaCl(OH), gradually neutralized and released into the liquid phase as HTT proceeded. In our experiments, it could achieve good chlorine removal with low clean water consumption.

In addition, the HMs were analyzed before and after the co-HTT of IFA and MSS. The addition of IFA enhanced the accumulation of HMs in MSS and improved their immobilization after HTT. As the total amount of HMs in the residue was still high, necessary measures should be taken for post-treatment extraction and reuse.

Acknowledgements

All the authors are grateful for the support provided by the Strategic Priority Research Program of the Chinese Academy of Sciences (Grant No. XDA23030301), the China-Japanese Research Cooperative Program-China (No. 2016YFE0118000) and the Scientific and Technology Major Special Project of Tianjin City (16YFXTSF00420).

Appendix A. Supplementary material

Supplementary data to this article can be found online at https://doi.org/10.1016/j.wasman.2019.09.006.

References

Ashok, J., Das, S., Yeo, T.Y., Dewangan, N., Kawi, S., 2018. Incinerator bottom ash derived from municipal solid waste as a potential catalytic support for biomass tar reforming. Waste Manag. 82, 249–257.
Berge, N.D., Ro, K.S., Mao, J., Flora, J.R., Chappell, M.A., Bae, S., 2011. Hydrothermal carbonization of municipal waste streams. Environ. Sci. Technol. 45, 5696–5703.
Chen, W.S., Chang, F.C., Shen, Y.H., Tsai, M.S., Ko, C.H., 2012. Removal of chloride from MSWI fly ash. J. Hazard. Mater. 237–238, 116–120.
Chen, X., Bi, Y., Zhang, H., Wang, J., 2016. Chlorides removal and control through water-washing process on MSWI Fly Ash. Procedia Environ. Sci. 31, 560–566.
Hu, Y., Yang, F., Chen, F., Feng, Y., Chen, D., Dai, X., 2018. Pyrolysis of the mixture of MSWI fly ash and sewage sludge for co-disposal: Effect of ferrous/ferric sulfate additives. Waste Manag. 75, 340–351.
Hu, Y., Zhang, P., Chen, D., Zhou, B., Li, J., Li, X.W., 2012. Hydrothermal treatment of municipal solid waste incineration fly ash for dioxin decomposition. J. Hazard. Mater. 207–208, 79–85.
Hu, Y., Zhang, P., Li, J., Chen, D., 2015. Stabilization and separation of heavy metals in incineration fly ash during the hydrothermal treatment process. J. Hazard. Mater. 299, 149–157.
Huang, H.J., Yuan, X.Z., 2016. The migration and transformation behaviors of heavy metals during the hydrothermal treatment of sewage sludge. Bioresour. Technol. 200, 991–998.
Jin, Y.-Q., Ma, X.-J., Jiang, X.-G., Liu, H.-M., Li, X.-D., Yan, J.-H., Cen, K.-F., 2012. Effects of hydrothermal treatment on the major heavy metals in fly ash from municipal solid waste incineration. Energy Fuels 27, 394–400.
Jing, Z., Fan, X., Zhou, L., Fan, J., Zhang, Y., Pan, X., Ishida, E.H., 2013. Hydrothermal solidification behavior of municipal solid waste incineration bottom ash without any additives. Waste Manag. 33, 1182–1189.
Kirby, C.S., Rimstidt, J.D., 1994. Interaction of municipal solid waste ash with water. Environ. Sci. Technol. 28, 443–451.
Kumar, M., Olajire Oyedun, A., Kumar, A., 2018. A review on the current status of various hydrothermal technologies on biomass feedstock. Renew. Sustain. Energy Rev. 81, 1742–1770.
Lederer, J., Trinkel, V., Fellner, J., 2017. Wide-scale utilization of MSWI fly ashes in cement production and its impact on average heavy metal contents in cements: the case of Austria. Waste Manag 60, 247–258.
Li, C., Wang, X., Zhang, G., Yu, G., Lin, J., Wang, Y., 2017. Hydrothermal and alkaline hydrothermal pretreatments plus anaerobic digestion of sewage sludge for dewatering and biogas production: Bench-scale research and pilot-scale verification. Water Res. 117, 49–57.
Liu, T., Liu, Z., Zheng, Q., Lang, Q., Xia, Y., Peng, N., Gai, C., 2018. Effect of hydrothermal carbonization on migration and environmental risk of heavy metals in sewage sludge during pyrolysis. Bioresour. Technol. 247, 282–290.
Liu, X., Lai, D., Wang, Y., 2019. Performance of Pb(II) removal by an activated carbon supported nanoscale zero-valent iron composite at ultralow iron content. J. Hazard. Mater. 361, 37–48.
Nowak, B., Frías Rocha, S., Aschenbrenner, P., Rechberger, H., Winter, F., 2012. Heavy metal removal from MSW fly ash by means of chlorination and thermal treatment: influence of the chloride type. Chem. Eng. J. 179, 178–185.
Pan, Y., Wu, Z., Zhou, J., Zhao, J., Ruan, X., Liu, J., Qian, G., 2013. Chemical characteristics and risk assessment of typical municipal solid waste incineration (MSWI) fly ash in China. J. Hazard. Mater. 261, 269–276.
Qi, X., Song, G., Yang, S., Yang, Z., Lyu, Q., 2018. Migration and transformation of sodium and chlorine in high-sodium high-chlorine Xinjiang lignite during circulating fluidized bed combustion. J. Energy Inst.
Qian, G., Cao, Y., Chui, P., Tay, J., 2006. Utilization of MSWI fly ash for stabilization/solidification of industrial waste sludge. J. Hazard. Mater. 129, 274–281.
Qiao, W., Wang, W., Wan, X., Xia, Z., Deng, Z., 2010. Improve sludge dewatering performance by hydrothermal treatment. J Residuals Sci Tech 7, 7–11.
Tang, J., Ylmén, R., Petranikova, M., Ekberg, C., Steenari, B.-M., 2018. Comparative study of the application of traditional and novel extractants for the separation of metals from MSWI fly ash leachates. J. Cleaner Prod. 172, 143–154.

Wang, L., Jin, Y., Nie, Y., Li, R., 2010. Recycling of municipal solid waste incineration fly ash for ordinary Portland cement production: a real-scale test. Resour. Conserv. Recycl. 54, 1428–1435.
Wang, L., Li, A., Chang, Y., 2016a. Hydrothermal treatment coupled with mechanical expression at increased temperature for excess sludge dewatering: Heavy metals, volatile organic compounds and combustion characteristics of hydrochar. Chem. Eng. J. 297, 1–10.
Wang, L., Zhang, L., Li, A., 2014. Hydrothermal treatment coupled with mechanical expression at increased temperature for excess sludge dewatering: influence of operating conditions and the process energetics. Water Res. 65, 85–97.
Wang, X., Chi, Q., Liu, X., Wang, Y., 2019. Influence of pyrolysis temperature on characteristics and environmental risk of heavy metals in pyrolyzed biochar made from hydrothermally treated sewage sludge. Chemosphere 216, 698–706.
Wang, X., Li, C., Zhang, B., Lin, J., Chi, Q., Wang, Y., 2016b. Migration and risk assessment of heavy metals in sewage sludge during hydrothermal treatment combined with pyrolysis. Bioresour. Technol. 221, 560–567.
Weidemann, E., Lundin, L., 2015. Behavior of PCDF, PCDD, PCN and PCB during low temperature thermal treatment of MSW incineration fly ash. Chem. Eng. J. 279, 180–187.
Xie, J., Hu, Y., Chen, D., Zhou, B., 2010. Hydrothermal treatment of MSWI fly ash for simultaneous dioxins decomposition and heavy metal stabilization. Front. Environ. Sci. Eng. China 4, 108–115.
Yang, Z., Tian, S., Ji, R., Liu, L., Wang, X., Zhang, Z., 2017. Effect of water-washing on the co-removal of chlorine and heavy metals in air pollution control residue from MSW incineration. Waste Manag 68, 221–231.
Ye, Y., Ngo, H.H., Guo, W., Liu, Y., Li, J., Liu, Y., Zhang, X., Jia, H., 2017. Insight into chemical phosphate recovery from municipal wastewater. Sci. Total Environ. 576, 159–171.
Yin, K., Gao, X., Sun, Y., Zheng, L., Wang, W., 2013. Thermal degradation of hexachlorobenzene in the presence of calcium oxide at 340–400 degrees C. Chemosphere 93, 1600–1606.
Youcai, Z., 2017. Municipal solid waste incineration process and generation of bottom ash and fly ash, pollution control and resource recovery. Municipal Solid Wastes Incineration, pp. 1–59.
Yu, J., Guo, M., Xu, X., Guan, B., 2014. The role of temperature and CaCl2 in activated sludge dewatering under hydrothermal treatment. Water Res. 50, 10–17.
Zhai, Y., Liu, X., Zhu, Y., Peng, C., Wang, T., Zhu, L., Li, C., Zeng, G., 2016. Hydrothermal carbonization of sewage sludge: the effect of feed-water pH on fate and risk of heavy metals in hydrochars. Bioresour. Technol. 218, 183–188.
Zhang, G., Wang, H., Xu, Y., Liu, Z., Xu, G., 2011. Enhanced improvement of sludge dewaterability by municipal solid waste incineration (MSWI) fly ash. Fresen Environ Bull 20, 1236–1244.
Zhang, Q., Hu, J., Lee, D.J., Chang, Y., Lee, Y.J., 2017. Sludge treatment: current research trends. Bioresour. Technol. 243, 1159–1172.
Zhu, F., Takaoka, M., Oshita, K., Morisawa, S., Tsuno, H., Kitajima, Y., 2009. Chloride behavior in washing experiments of two kinds of municipal solid waste incinerator fly ash with different alkaline reagents. J. Air Waste Manag. Assoc. 59, 139–147.
Zhu, F., Takaoka, M., Shiota, K., Oshita, K., Kitajima, Y., 2008. Chloride Chemical form in various types of fly ash. Environ. Sci. Technol. 42, 3932–3937.